International Journal of Control, Automation and Systems 17(5) (2019) 1221-1232
http://dx.doi.org/10.1007/s12555-017-0322-9
ISSN:1598-6446 eISSN:2005-4092
http://www.springer.com/12555

Optimal Discrete-time Integral Sliding Mode Control for Piecewise Affine Systems

Olfa Jedda* and **Ali Douik**

Abstract: This paper presents an optimal discrete-time integral sliding mode control for constrained piecewise affine systems. The proposed scheme is developed on the basis of linear quadratic regulator approach and differential evolution algorithm in order to ensure the stability of the closed-loop system in discrete-time sliding mode and the optimization of response characteristics in presence of control input constraints. Moreover, the controller is designed such that chattering phenomenon is avoided and finite-time convergence to the sliding surface is guaranteed. The follow-up of a reference model is also ensured. The efficiency of the proposed method is illustrated with an inverted pendulum system.

Keywords: Differential evolution algorithm, discrete-time integral sliding mode control, inverted pendulum system, piecewise affine systems.

1. INTRODUCTION

Over the last few decades, research activities in computer science and control have been strongly oriented to study hybrid dynamical systems since they are used for modeling the behaviour of realistic complex systems. In fact, they involve explicitly and simultaneously continuous and discrete dynamics. In other words, discrete processes are employed to select, control and supervise the behaviour of continuous processes [1]. Several subclasses of hybrid dynamical systems, such as linear complementarity (LC) systems [2, 3], mixed logical dynamical (MLD) systems [4], piecewise affine (PWA) systems [5], and max-min-plus-scaling systems (MMPS) [6], are established in literature in order to make possible analysis and development of control techniques which are not available for general hybrid systems.

Recently, piecewise affine systems have received much attention in research not only because they can provide a useful modeling method for a large category of hybrid dynamical systems but also because they can be used to approximate nonlinear systems, given that they are equivalent to interconnections of linear systems and finite automata [7]. Moreover, all techniques developed for PWA systems can be extended to some other subclasses, such as MLD systems [8], since they are equivalent as demonstrated by Heemls *et al*. in [9].

Numerous research studies concerning PWA discrete-time systems have been carried out on stability criteria [10, 11], identification techniques [12, 13], and control methods such as optimal control [4, 14] and model predictive control (MPC) [4, 15]. In this paper, we propose a new control technique for PWA discrete-time systems based on discrete-time sliding mode theory.

Discrete-time sliding mode control (DSMC) appeared in the mid 1980s with Milosavljevic [16] and then has been followed with a great interest from control community [17–21] in view of the increasing use of computers for the implementation of digital controllers. Yet, invariance and robustness properties of continuous-time sliding mode control (CSMC) against parametric uncertainties, modeling errors and external disturbances [22–25] can not be maintained in discrete-time because of the finite sampling rate. Actually, the control input is updated at each sampling time so that it can not be changed when the state trajectory crosses the sliding surface during the sampling period; hence the occurrence of chattering phenomenon that may excite high-frequency dynamics, adversely affect system performance and damage electric power circuits and mechanical parts.

In [19], Gao introduced the notion of quasi-sliding mode that consists in bringing the state trajectory to cross the sliding surface in finite-time and therefore to follow a zigzag motion within a boundary layer in its vicinity so that the chatter effect will be attenuated but not totally avoided. In [26], Bartolini *et al*. developed a discrete-time control algorithm that consists in defining the equivalent control as the piecewise-constant control that guarantees

Manuscript received June 5, 2017; revised April 28, 2018; accepted January 20, 2019. Recommended by Associate Editor Tae-Hyoung Kim under the direction of Editor Euntai Kim.

Olfa Jedda is with the Electrical Engineering Department, National Engineering School of Monastir, University of Monastir, Tunisia (e-mail: olfa_jedda@outlook.com). Ali Douik is with the Computer Engineering Department, National Engineering School of Sousse, University of Sousse, Tunisia (e-mail: ali.douik@enim.rnu.tn).
* Corresponding author.

the elimination of chattering phenomenon as well as the occurrence of an ideal discrete-time sliding mode in finite-time.

Later, discrete-time integral sliding mode control (DISMC) was proposed by Abidi *et al.* in [27] as an improved approach of DSMC based on the integral sliding mode concept [28]. Recently, it was developed for robust tracking and model following of uncertain systems [29, 30] and systems with state and input delays [31, 32]. In addition to its straightforward design, DISMC controller ensures the elimination of reaching phase, the stability of the closed-loop system, the excellent tracking performance and the high degree of accuracy. Moreover, in quasi-sliding mode, the motion equation has the same order as the state space instead of being reduced by the dimension of the control input as is the case with the conventional sliding mode controller. Yet, the integral term of the sliding function is at the origin of error accumulation in the initial phase and therefore of high values of control input. In presence of control input constraints in practical application, this can cause uncontrollable overshoots, oscillations and even instability which may be the origin of an unanticipated deterioration of control devices.

In what follows, an optimal discrete-time integral sliding mode control (ODISMC) will be developed for PWA systems subject to input constraints. Actually, the linear quadratic regulator (LQR) approach and the differential evolution (DE) algorithm are used in the sliding function design in order to ensure the stability of the closed-loop system in discrete-time sliding mode and the optimum response characteristics while respecting control input constraints. Proposed by Storn and Price [33], the differential evolution algorithm is a stochastic population-based optimization method that has been widely applied in various scientific and engineering domains [34]. It has many advantages such as simplicity of implementation, reduced number of control parameters and efficiency in finding the global minimum of non-differentialble, discontinuous and nonlinear cost functions [35–37].

The proposed controller will be applied to an inverted pendulum system modeled as a single-input single-output PWA system with input constraints. It will be compared to optimal discrete-time integral sliding mode controller using linear matrix inequality (LMI) approach, to discrete-time integral sliding mode controller based on an arbitrary selection of the sliding vectors, and therefore to model predictive controller in order to demonstrate its efficiency.

This paper is organized as follows: Section 2 is devoted to the design of optimal discrete-time integral sliding mode controller for constrained piecewise affine systems. A discrete-time PWA model of an inverted pendulum system is given in Section 3. Section 4 presents the numerical simulation results as well as their comparison to results of other methods. Finally, concluding remarks are provided in Section 5.

2. OPTIMAL DISCRETE-TIME INTEGRAL SLIDING MODE CONTROL FOR PWA SYSTEMS

The PWA systems are defined as the partition of the state space into a finite number of polyhedral regions such that a different affine state-updated equation is associated with each region. They are described by

$$\begin{aligned} x(k+1) &= A_i x(k) + B_i u(k) + f_i, \\ y(k) &= C_i x(k) + D_i u(k) + h_i, \end{aligned} \quad \text{if } \begin{bmatrix} x(k) \\ u(k) \end{bmatrix} \in \Omega_i, \tag{1}$$

where $x(k) \in \mathbb{R}^n$ is the state vector, $u(k) \in \mathbb{R}^m$ is the control input, and $y(k) \in \mathbb{R}^p$ is the system output. Ω_i are convex polyhedra in the state/input space given by

$$\Omega_i = \left\{ \begin{bmatrix} x(k) \\ u(k) \end{bmatrix} \in \mathbb{R}^{n+m} : N_i x + L_i u \le E_i \right\}, \quad i = 1 \dots ns, \tag{2}$$

where ns is the number of subsystems. A_i, B_i, f_i, C_i, D_i, h_i, N_i, L_i and E_i are constant matrices of appropriate dimensions [9, 38–41].

In order to make the notation in the following development less cluttered, each subsystem is expressed as follows

$$\begin{cases} x(k+1) = Ax(k) + Bu(k) + f, \\ y(k) = Cx(k) + Du(k) + h, \end{cases} \tag{3}$$

where $(u(k), y(k)) \in \mathbb{R} \times \mathbb{R}$ and both matrices (D, h) are supposed to be equal to 0 in this study.

The discrete-time reference model is given by

$$\begin{cases} x_m(k+1) = A_m x_m(k), \\ y_m(k) = C_m x_m(k), \end{cases} \tag{4}$$

where $x_m(k) \in \mathbb{R}^{n_m}$ is the state vector and $y_m(k)$ is the reference model output that has the same dimension as $y(k)$.

According to [32, 42, 43], tracking the reference output $y_m(k)$ requires the existence of matrices $G \in \mathbb{R}^{n \times n_m}$ and $H \in \mathbb{R}^{1 \times n_m}$ that satisfy the following relation

$$\begin{bmatrix} A & B \\ C & 0 \end{bmatrix} \begin{bmatrix} G \\ H \end{bmatrix} = \begin{bmatrix} GA_m \\ C_m \end{bmatrix}. \tag{5}$$

If there is no solution for (5), one must choose a different reference model (A_m,C_m) or system output matrix C [42].

Consider that the tracking controller has the following structure

$$u(k) = Hx_m(k) + v(k), \tag{6}$$

where H fulfills condition (5) and $v(k)$ is defined as an auxiliary control law. Then, an auxiliary state vector $z(k)$ will be introduced in order to facilitate the development of the proposed scheme. It is defined as

$$z(k) = x(k) - Gx_m(k), \tag{7}$$

where G satisfies condition (5).

Using (3) and (7), the auxiliary subsystem can be expressed as follows

$$z(k+1) = Az(k) + Bv(k) + f. \tag{8}$$

Later, the ODISMC controller is used to design the auxiliary control law $v(k)$ such that the system output $y(k)$ follows the reference model output $y_m(k)$, the auxiliary subsystem (8) is asymptotically stable in discrete-time sliding mode, and the response characteristics are optimized in presence of control input constraints.

2.1. Design of optimal integral sliding surface

The integral sliding function is defined as

$$\sigma(k) = Sz(k) - S\exp(-\beta k)z(0) - \varepsilon(k), \quad \beta > 0, \tag{9a}$$
$$\varepsilon(k) = \varepsilon(k-1) + S(A+BK)z(k-1), \quad \varepsilon(0) = 0, \tag{9b}$$

where $S \in \mathbb{R}^{1\times n}$ is determined using the differential evolution algorithm while ensuring that SB is non-singular and $K \in \mathbb{R}^{1\times n}$ is designed using the linear quadratic regulator approach in order to ensure the stability of the auxiliary subsystem (8) in discrete-time sliding mode and the optimization of response characteristics.

2.1.1 Differential evolution algorithm

Given that for each subsystem the sliding vector is expressed as $S = \left[s^1, \ldots, s^n\right]$, the DE algorithm is used to generate the global optimum vector $\Xi = \left[\xi^1, \ldots, \xi^{nt}\right] = \left[s_1^1, \ldots, s_1^n, \ldots, s_{ns}^1, \ldots, s_{ns}^n\right]$ that minimizes the following cost function

$$cost = \lambda_1 t_r + \lambda_2 t_s + \lambda_3 M_p + \lambda_4 E_{ss}, \tag{10}$$

where t_r is the rise-time, t_s is the settling-time, M_p is the overshoot, E_{ss} is the steady-state error, and λ_q , $q = 1, \ldots, 4$, are their corresponding weights.

DE starts with a population of NP nt-dimensional parameter vectors $\Xi_{j,Gen} = \left[\xi_{j,Gen}^1, \ldots, \xi_{j,Gen}^{nt}\right]$, $j = 1, \ldots, NP$. In presence of search space constraints $\Xi_{max} = \left[\xi_{max}^1, \ldots, \xi_{max}^{nt}\right]$ and $\Xi_{min} = \left[\xi_{min}^1, \ldots, \xi_{min}^{nt}\right]$, each parameter in the j^{th} vector of the initial generation $Gen = 0$ is generated as follows:

$$\xi_{j,0}^{\delta} = \xi_{min}^{\delta} + rand\,(0,1)\left(\xi_{max}^{\delta} - \xi_{min}^{\delta}\right), \quad \delta = 1, \ldots, nt, \tag{11}$$

where $rand\,(0,1)$ returns a random number that is uniformly distributed over the interval $[0,1]$.

Then, a mutant vector $\Phi_{j,Gen} = \left[\phi_{j,Gen}^1, \ldots, \phi_{j,Gen}^{nt}\right]$ is created for each individual $\Xi_{j,Gen}$ via the mutation strategy DE/best/1 described by

$$\Phi_{j,Gen} = \Xi_{best,Gen} + F\left(\Xi_{r_1^j,Gen} - \Xi_{r_2^j,Gen}\right). \tag{12}$$

Different from the index j, the integers r_1^j and r_2^j are randomly generated within the range $[1, NP]$. $F \in [0,2]$ is the scaling factor fixed during the optimization process, and $\Xi_{best,Gen}$ is the best individual corresponding to the least cost function value at the current generation Gen.

Next, DE employs the crossover operation for each target vector $\Xi_{j,Gen}$ and its corresponding mutant vector $\Phi_{j,Gen}$ in order to increase the potential of the population diversity. A trial vector $\Psi_{j,Gen} = \left[\psi_{j,Gen}^1, \ldots, \psi_{j,Gen}^{nt}\right]$ is generated on the basis of the binomial crossover scheme defined by

$$\psi_{j,Gen}^{\delta} = \begin{cases} \phi_{j,Gen}^{\delta} & \text{if } rand_{\delta}\,(0,1) \le CR \\ & \text{or } \delta = \delta_{rand}, \\ \xi_{j,Gen}^{\delta} & \text{otherwise,} \end{cases}$$
$$\delta = 1, \ldots, nt, \tag{13}$$

where CR is the crossover rate chosen constant within the range $[0,1]$ and δ_{rand} is randomly chosen within the range $[1, nt]$. If there is any parameter value of the trial vector that exceeds the minimum and maximum bounds set in advance, it will be uniformly and randomly reinitialized in the search space.

Subsequently, DE uses a selection process that consists in comparing the cost function value of each trial vector $\Psi_{j,Gen}$ with that of its corresponding target vector $\Xi_{j,Gen}$. Actually, if the cost function value of the trial vector is less or equal to that of the target vector, the latter will be replaced by the trial vector in the next generation. Otherwise, it will remain for the next generation. This operation can be expressed as follows:

$$\Xi_{j,Gen+1} = \begin{cases} \Psi_{j,Gen} & \text{if } cost\,(\Psi_{j,Gen}) \le cost\,(\Xi_{j,Gen}), \\ \Xi_{j,Gen} & \text{otherwise.} \end{cases} \tag{14}$$

Moreover, a fixed number ρ of sliding vectors that correspond to the worst cost function values will be replaced, at each generation, by those corresponding to the best fitness values. This operation aims to accelerate the convergence of this algorithm by preventing the worst individuals to get involved in the other operations.

As shown in Table 1, all the above-mentioned operations will be repeated generation after generation until the satisfaction of certain criteria [34, 44].

2.1.2 Linear quadratic regulator approach

Let's consider a forward expression of the sliding function given in (9)

$$\sigma(k+1) = Sz(k+1) - S\exp(-\beta(k+1))z(0) - \varepsilon(k+1), \tag{15a}$$
$$\varepsilon(k+1) = \varepsilon(k) + S(A+BK)z(k). \tag{15b}$$

Table 1. Description of DE algorithm.

Step 1	Set the population size NP, the scale factor $F \in [0,2]$, and the crossover rate $CR \in [0,1]$.
Step 2	**Initialization** Set the generation number $Gen = 0$. Initialize randomly and uniformly a population of NP individuals $\Xi_{j,Gen} = \left[\xi^1_{j,Gen}, \dots, \xi^{nt}_{j,Gen}\right]$, $j = 1,\dots,NP$, within the maximum and minimum bounds $\Xi_{max} = \left[\xi^1_{max}, \dots, \xi^{nt}_{max}\right]$ and $\Xi_{min} = \left[\xi^1_{min}, \dots, \xi^{nt}_{min}\right]$. FOR $j = 1$ to NP FOR $\delta = 1$ to nt $\xi^\delta_{j,0} = \xi^\delta_{min} + rand\,(0,1)\left(\xi^\delta_{max} - \xi^\delta_{min}\right)$ END FOR END FOR Evaluate the initial population individuals.

Step 3	WHILE stop criterion is not satisfied DO
	Select the best individual $\Xi_{best,Gen}$ that corresponds to the best cost function value.
	Replace a fixed number ρ of sliding vectors that correspond to the worst cost function values by those corresponding to the best ones.
	FOR $j = 1$ to NP
	Step 3.1 Mutation operation
	Select randomly 2 distinct indexes r^j_1 and r^j_2 from the range $\{1,\dots,NP\} \setminus \{j\}$.
	Generate the mutant vector $\Phi_{j,Gen} = \left[\phi^1_{j,Gen}, \dots, \phi^{nt}_{j,Gen}\right]$ that corresponds to the target vector $\Xi_{j,Gen}$.
	$\Phi_{j,Gen} = \Xi_{best,Gen} + F\left(\Xi_{r^j_1,Gen} - \Xi_{r^j_2,Gen}\right)$
	Step 3.2 Crossover operation
	Generate the trial vector. $\Psi_{j,Gen} = \left[\psi^1_{j,Gen}, \dots, \psi^{nt}_{j,Gen}\right]$ for each target vector $\Xi_{j,Gen}$ and its corresponding mutant vector $\Phi_{j,Gen}$.
	$\delta_{rand} = \lfloor rand\,(0,1) \times nt \rfloor$
	FOR $\delta = 1$ to nt
	IF $(rand_\delta \le CR)$ or $(\delta = \delta_{rand})$
	$\psi^\delta_{j,Gen} = \phi^\delta_{j,Gen}$
	ELSE
	$\psi^\delta_{j,Gen} = \xi^\delta_{j,Gen}$
	END IF
	END FOR
	Step 3.3 Selection operation
	Evaluate the trial vector $\Psi_{j,Gen}$
	IF $cost\,(\Psi_{j,Gen}) \le cost\,(\Xi_{j,Gen})$ THEN
	$\Xi_{j,Gen+1} = \Psi_{j,Gen}$
	else
	$\Xi_{j,Gen+1} = \Xi_{j,Gen}$
	end if
	END FOR
	Increment the generation count
	$Gen = Gen + 1$
	END WHILE

Using the equivalent control approach, the equivalent control v_{eq} is obtained by setting $\sigma(k+1) = 0$. Then, it can be expressed as follows

$$\begin{aligned} v_{eq}(k) =& Kz(k) - (SB)^{-1}Sf + (SB)^{-1}S\exp(-\beta(k+1))z(0) \\ &+ (SB)^{-1}\varepsilon(k). \end{aligned} \tag{16}$$

In discrete-time sliding mode, solving $\sigma(k) = 0$ leads to

$$\varepsilon(k) = Sz(k) - S\exp(-\beta k)z(0). \tag{17}$$

Substituting (17) into (16) yields

$$v_{eq}(k) = Kz(k) + (SB)^{-1}Sz(k) - (SB)^{-1}Sf + \Gamma(k), \tag{18}$$

where

$$\Gamma(k) = (SB)^{-1}S[\exp(-\beta(k+1)) - \exp(-\beta k)]z(0). \tag{19}$$

Consequently, the auxiliary subsystem in discrete-time sliding mode can be expressed as follows:

$$z(k+1) = A_c z(k) + d(k), \tag{20}$$

where $A_c = A + B(SB)^{-1}S + BK$ and $d(k) = (I - B(SB)^{-1}S)f + B\Gamma(k)$.

Remark 1: The exponential term $\Gamma(k)$ given in (19) tends towards zero when k approaches infinity and then the last term $d(k)$ in (20) tends towards the constant term $(I - B(SB)^{-1}S)f$, i.e. $\lim_{k\to\infty} d(k) = (I - B(SB)^{-1}S)f$. Thus, $d(k)$ will not affect the stability of the auxiliary subsystem (20) in discrete-time sliding mode. In addition, if $(I - B(SB)^{-1}S)f \equiv 0$, the auxiliary subsystem (20) is asymptotically stable in discrete-time sliding mode.

In what follows, the gain vector K will be designed using the infinite time horizon discrete-time LQR in order to ensure the stability of the equilibrium of the auxiliary subsystem (20) in discrete-time sliding mode.

Theorem 1: The equilibrium of the auxiliary subsystem (20) is asymptotically stable in discrete-time sliding mode if there exist a positive-definite matrix $P \in \mathbb{R}^n$ such that the following inequality is satisfied

$$A_c^T P A_c - P < 0. \tag{21}$$

Proof: Firstly, a positive definite Lyapunov function is chosen as follows

$$V(k) = z^T(k)Pz(k). \tag{22}$$

The Lyapunov difference of the auxiliary subsystem (20) without the last term $d(k)$ is expressed by

$$\begin{aligned} \Delta V(k) &= V(k+1) - V(k) \\ &= z^T(k+1)Pz(k+1) - z^T(k)Pz(k) \\ &= z^T(k)\left(A_c^T P A_c - P\right)z(k). \end{aligned} \tag{23}$$

The stability requires that $\Delta V(k)$ is negative-definite and this is only possible if $A_c^T P A_c - P < 0$ as required by (21). Then, the equilibrium of the auxiliary subsystem (20) is asymptotically stable in the sense of Lyapunov stability in discrete-time sliding mode. The proof is completed. □

Theorem 2: The equilibrium of the auxiliary subsystem (20) is asymptotically stable in discrete-time sliding mode if there exist positive-definite matrices $Q \in \mathbb{R}^n$ and $R \in \mathbb{R}$ such that the LQR infinite horizon objective function given by

$$J = \sum_{k=0}^{\infty} (z(k)^T Q z(k) + v_{eq}(k)^T R v_{eq}(k)) \tag{24}$$

is minimized. The feedback gain K is given by

$$K = (B_{eq}^T P B_{eq} + R)^{-1} B_{eq}^T P A_{eq}, \tag{25}$$

where $A_{eq} = A + B(SB)^{-1} S$, $B_{eq} = -B$ and P is a positive-definite matrix solution of the discrete-time algebraic Riccati equation

$$\begin{aligned} &A_{eq}^T P A_{eq} - P - A_{eq}^T P B_{eq} (B_{eq}^T P B_{eq} + R)^{-1} B_{eq}^T P A_{eq} + Q \\ &= 0. \end{aligned} \tag{26}$$

Proof:

$$\begin{aligned} &A_c^T P A_c - P \\ &= (A_{eq} - B_{eq} K)^T P (A_{eq} - B_{eq} K) - P \\ &= A_{eq}^T P A_{eq} - A_{eq}^T P B_{eq} K - K^T B_{eq}^T P A_{eq} \\ &\quad + K^T B_{eq}^T P B_{eq} K - P \\ &= \left(A_{eq}^T P A_{eq} - P - A_{eq}^T P B_{eq} K + Q\right) - Q \\ &\quad - K^T B_{eq}^T P A_{eq} + K^T \left(B_{eq}^T P B_{eq} + R\right) K - K^T R K \\ &= \left(A_{eq}^T P A_{eq} - P - A_{eq}^T P B_{eq} K + Q\right) \\ &\quad - Q - K^T R K - K^T \left(B_{eq}^T P B_{eq} + R\right) \\ &\quad \times \left[\left(B_{eq}^T P B_{eq} + R\right)^{-1} B_{eq}^T P A_{eq} - K\right]. \end{aligned}$$

Replacing K by its expression given in (25) yields

$$A_c^T P A_c - P = -Q - K^T R K < 0. \tag{27}$$

From Theorem 1, it concludes that the existence of P satisfying Riccati equation (26) guarantees the stability of the equilibrium of the auxiliary subsystem (20) in discrete-time sliding mode, and the gain vector K can be expressed as in (25). The proof is completed. □

2.1.3 Analysis of overall system stability

For each region, the auxiliary subsystem in discrete-time sliding mode is given by

$$z(k+1) = A_{ci} z(k) + d_i(k), \quad i = 1 \ldots ns, \tag{28}$$

where $A_{ci} = A_i + B_i(S_iB_i)^{-1}S_i + B_iK_i$, $d_i(k) = (I - B_i(S_iB_i)^{-1}S_i)f_i + B_i\Gamma_i(k)$, and $\Gamma_i(k) = (S_iB_i)^{-1}S_i[\exp(-\beta(k+1)) - \exp(-\beta k)]z(0)$. S_i and K_i are respectively the sliding and gain vectors determined previously using DE algorithm and LQR approach.

The connection of all auxiliary subsystems is stable in discrete-time sliding mode if there exist a positive-definite matrix $P \in \mathbb{R}^n$ such that for each region the Lyapunov function V (22) is positive-definite and the Lyapunov difference ΔV (23) is negative-definite.

2.2. Design of optimal discrete-time integral sliding mode controller

In this paper, The control law will be designed such that the chattering phenomenon is eliminated and the state trajectory converges to the sliding surface after a finite time interval. Control input constraints are taken into account in the control design.

The forward expression of the sliding function (9) can be rewritten as follows :

$$\begin{aligned} \sigma(k+1) = &\sigma(k) - (S + SBK) z(k) + SBv(k) + Sf \\ &- SB\Gamma(k). \end{aligned} \tag{29}$$

Hence, the corresponding equivalent auxiliary control is expressed as

$$\begin{aligned} v_{eq}(k) = &-(SB)^{-1}\sigma(k) + \left((SB)^{-1}S + K\right) z(k) \\ &- (SB)^{-1}Sf + \Gamma(k). \end{aligned} \tag{30}$$

Considering that the control input $u(k)$ may vary within the admissible domain $[-u_0, u_0]$, i.e. $\|u(k)\| \le u_0$, the auxiliary control must belong to the range $[v_{min}, v_{max}]$ with $v_{min} = -u_0 - Hx_m$ and $v_{max} = u_0 - Hx_m$. The constrained auxiliary control is given by

$$v(k) = \begin{cases} v_{eq}(k) & \text{if } v_{min} \le v_{eq}(k) \le v_{max}, \\ v_{max} & \text{if } v_{eq}(k) > v_{max}, \\ v_{min} & \text{if } v_{eq}(k) < v_{min}. \end{cases} \tag{31}$$

Suppose that $\|Hx_m\| < u_0$, $\|v(k)\| \le v_0$ and

$$\|(SB)^{-1}\| \| (S + SBK) z(k) - Sf + SB\Gamma(k)\| < v_0, \tag{32}$$

where $v_0 = \min(\|v_{min}\|, \|v_{max}\|)$.

In this restrained domain, the constrained auxiliary control can be expressed as follows:

$$v(k) = \begin{cases} v_{eq}(k) & \text{if } \|v_{eq}(k)\| \le v_0, \\ v_0 \dfrac{v_{eq}(k)}{\|v_{eq}(k)\|} & \text{if } \|v_{eq}(k)\| > v_0. \end{cases} \tag{33}$$

Using (30), the forward expression of the sliding function

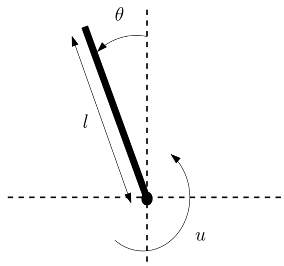

Fig. 1. Schematic of the inverted pendulum system.

(29) for $\|v_{eq}(k)\| > v_0$ is given by

$$\sigma(k+1) = (\sigma(k) - (S+SBK)z(k) + Sf - SB\Gamma(k)) \times \left(1 - \frac{v_0}{\|v_{eq}(k)\|}\right). \tag{34}$$

Therefore, using (32)

$$\begin{aligned}
&\|\sigma(k+1)\| \\
&= \|\sigma(k) - (S+SBK)z(k) + Sf - SB\Gamma(k)\| \\
&\quad - v_0 \frac{\|\sigma(k) - (S+SBK)z(k) + Sf - SB\Gamma(k)\|}{\|v_{eq}(k)\|} \\
&\leq \|\sigma(k)\| + \|(S+SBK)z(k) - Sf + SB\Gamma(k)\| \\
&\quad - v_0 \frac{\|\sigma(k) - (S+SBK)z(k) + Sf - SB\Gamma(k)\|}{\|(SB)^{-1}\| \|\sigma(k) - (S+SBK)z(k) + Sf - SB\Gamma(k)\|} \\
&\leq \|\sigma(k)\| + \|(S+SBK)z(k) - Sf + SB\Gamma(k)\| \\
&\quad - \frac{v_0}{\|(SB)^{-1}\|} \\
&< \|\sigma(k)\|.
\end{aligned}$$

Thus a monotonic decrease of $\|\sigma(k)\|$ occurs. Moreover, the equivalent auxiliary $v_{eq}(k)$ will belong to the restrained domain, i.e. $\|v_{eq}(k)\| \leq v_0$, and therefore to the admissible domain $[v_{min}, v_{max}]$, after a finite time interval. This can happen, according to (30) and (32), when $\sigma(k) = 0$. In other words, the state trajectory will converge to the sliding surface after a finite number of steps; hence the existence of discrete-time sliding mode.

3. PWA MODEL OF THE INVERTED PENDULUM SYSTEM

The schematic presentation of the inverted pendulum system given in Fig. 1 shows a simple pendulum of mass $M = 1$ kg and length $l = 0.5$ m rotated through an angle θ from the upright position by an input torque u. Actually, the input torque lies within a range of $u_{min} = -10$ Nm to $u_{max} = 10$ Nm. The pendulum is subject to gravity and viscous friction torque [38].

Let $x = \begin{bmatrix} x_1 & x_2 \end{bmatrix}^T = \begin{bmatrix} \theta & \dot{\theta} \end{bmatrix}^T$ be the state vector. The dynamic equations of the inverted pendulum are:

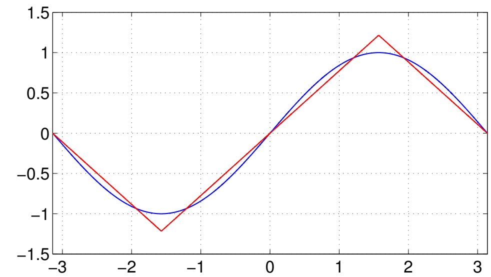

Fig. 2. Piecewise linear approximation of sine function over the interval $[-\pi\ \pi]$.

$$\begin{cases} \dot{x}_1 = x_2, \\ \dot{x}_2 = \dfrac{Mgl\sin x_1 - \tau x_2}{l^2 M} + \dfrac{1}{l^2 M}u, \end{cases} \tag{35}$$

where $g = 9.8\ \mathrm{m/s^2}$ is the acceleration of gravity and $\tau = 0.5$ Nms is the friction coefficient.

Referring to Fig. 2, the sine function is approximated over the interval $[-\pi\ \pi]$ by the following piecewise linear function

$$\sin\theta \approx \begin{cases} -\alpha\theta - \gamma & \text{if } \theta < -\frac{\pi}{2}, \\ \alpha\theta & \text{if } |\theta| \leq \frac{\pi}{2}, \\ -\alpha\theta + \gamma & \text{if } \theta > \frac{\pi}{2} \end{cases} \tag{36}$$

with $\alpha = \frac{24}{\pi^3}$ and $\gamma = \frac{24}{\pi^2}$.

Thus, replacing the sine function by its piecewise linear approximation in (35) and using, for discretization, the Euler forward method defined by

$$\dot{x} \cong \frac{x(k+1) - x(k)}{T_s} \tag{37}$$

yields the following discrete-time piecewise affine model

$$\begin{aligned} x(k+1) &= A_i x(k) + B_i u(k) + f_i, \quad i = 1, \dots, 3, \\ y(k) &= C_i x(k) \end{aligned} \tag{38}$$

with

$$\begin{cases}
A_1 = \begin{bmatrix} 1 & T_s \\ -\frac{T_s g\alpha}{l} & 1 - \frac{T_s\tau}{l^2 M} \end{bmatrix}, \quad B_1 = \begin{bmatrix} 0 \\ \frac{T_s}{l^2 M} \end{bmatrix}, \\
\qquad f_1 = \begin{bmatrix} 0 \\ -\frac{g\gamma T_s}{l} \end{bmatrix}, \quad C_1 = \begin{bmatrix} 1 & 0 \end{bmatrix}, \quad \text{if } \theta < -\dfrac{\pi}{2}, \\
A_2 = \begin{bmatrix} 1 & T_s \\ \frac{T_s g\alpha}{l} & 1 - \frac{T_s\tau}{l^2 M} \end{bmatrix}, \quad B_2 = \begin{bmatrix} 0 \\ \frac{T_s}{l^2 M} \end{bmatrix}, \\
\qquad f_2 = \begin{bmatrix} 0 \\ 0 \end{bmatrix}, \quad C_2 = \begin{bmatrix} 1 & 0 \end{bmatrix}, \quad \text{if } |\theta| \leq \dfrac{\pi}{2}, \\
A_3 = \begin{bmatrix} 1 & T_s \\ -\frac{T_s g\alpha}{l} & 1 - \frac{T_s\tau}{l^2 M} \end{bmatrix}, \quad B_3 = \begin{bmatrix} 0 \\ \frac{T_s}{l^2 M} \end{bmatrix}, \\
\qquad f_3 = \begin{bmatrix} 0 \\ \frac{g\gamma T_s}{l} \end{bmatrix}, \quad C_3 = \begin{bmatrix} 1 & 0 \end{bmatrix}, \quad \text{if } \theta > \dfrac{\pi}{2}.
\end{cases}$$

4. SIMULATION RESULTS

For a sampling period $T_s = 0.05$ s, the discrete-time reference model is given by

$$\begin{cases} x_m(k+1) = \begin{bmatrix} 1 & 0 \\ 0 & 1 \end{bmatrix} x_m(k), \\ y_m(k) = \begin{bmatrix} 1 & 0 \end{bmatrix} x_m(k). \end{cases} \tag{39}$$

The aim is to move the pendulum from the stable equilibrium position $\theta = \pi$ to the unstable equilibrium position $\theta = 0$ and maintain it there. Hence, the initial conditions for (38) and (39) are chosen as follows

$$x(0) = \begin{bmatrix} \pi & 0 \end{bmatrix}^T, \; x_m(0) = \begin{bmatrix} 0 & 0 \end{bmatrix}^T \tag{40}$$

The matrices G and H, solutions of (5), are given for each region by

$$\begin{cases} G_1 = \begin{bmatrix} 1 & 0 \\ 0 & 0 \end{bmatrix}, \; H_1 = \begin{bmatrix} 3.7967 & 0 \end{bmatrix} & \text{if } \theta < -\frac{\pi}{2}, \\ G_2 = \begin{bmatrix} 1 & 0 \\ 0 & 0 \end{bmatrix}, \; H_2 = \begin{bmatrix} -3.7967 & 0 \end{bmatrix} & \text{if } |\theta| \le \frac{\pi}{2}, \\ G_3 = \begin{bmatrix} 1 & 0 \\ 0 & 0 \end{bmatrix}, \; H_3 = \begin{bmatrix} 3.7967 & 0 \end{bmatrix} & \text{if } \theta > \frac{\pi}{2}. \end{cases} \tag{41}$$

The design parameter β in the sliding surface is equal to 0.9. The cost function to minimize using DE algorithm is chosen as follows:

$$cost = t_r + t_s. \tag{42}$$

The population size, the mutation scale factor and the crossover rate are respectively chosen as $NP = 100$, $F = 0.5$ and $CR = 0.9$.
The minimum and the maximum bounds are given by

$$\begin{aligned} \Xi_{min} &= \begin{bmatrix} 0.5 & 0.5 & 0.5 & 0.5 & 0.5 & 0.5 \end{bmatrix}, \\ \Xi_{max} &= \begin{bmatrix} 5 & 5 & 5 & 5 & 5 & 5 \end{bmatrix}. \end{aligned} \tag{43}$$

For LQR approach, the weighting matrices R and Q in (24) are selected for all subsystems as follows:

$$R_i = 1, Q_i = \begin{bmatrix} 1 & 0 \\ 0 & 1 \end{bmatrix}, \; i = 1, \ldots 3. \tag{44}$$

Fig. 3 illustrates the evolution of the cost function (42) for ODISMC using LQR approach. It reveals the rapid convergence of the cost function to its minimum value 1.01 s. This is due to the last operation added in the DE algorithm that consists in substituting a fixed number ρ, which is chosen equal to 5, of sliding vectors corresponding to the worst fitness value by those corresponding to the best cost value at each generation. The sliding vectors

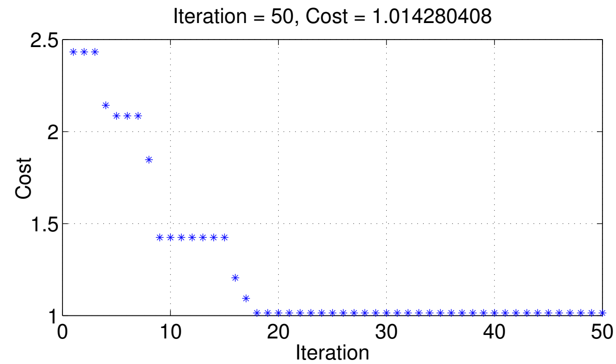

Fig. 3. Evolution of the cost function for ODISMC using LQR approach.

corresponding to the minimum value of the cost function (42) are given by

$$\begin{cases} S_1 = \begin{bmatrix} 1.9710 & 4.432 \end{bmatrix} & \text{if } \theta < -\frac{\pi}{2}, \\ S_2 = \begin{bmatrix} 5 & 1.3056 \end{bmatrix} & \text{if } |\theta| \le \frac{\pi}{2}, \\ S_3 = \begin{bmatrix} 2.5291 & 0.5 \end{bmatrix} & \text{if } \theta > \frac{\pi}{2}. \end{cases} \tag{45}$$

The obtained gain vectors using LQR approach are

$$\begin{cases} K_1 = \begin{bmatrix} 0.6088 & -6.9846 \end{bmatrix} & \text{if } \theta < -\frac{\pi}{2}, \\ K_2 = \begin{bmatrix} -33.7849 & -8.1815 \end{bmatrix} & \text{if } |\theta| \le \frac{\pi}{2}, \\ K_3 = \begin{bmatrix} -31.7025 & -8.1141 \end{bmatrix} & \text{if } \theta > \frac{\pi}{2}. \end{cases} \tag{46}$$

Let's suppose that $x_1 \in [-\pi, \pi]$ and $x_2 \in [-10, 10]$. According to equations (7), (40) and (41), the auxiliary state variables z_1 and z_2 are respectively within the same ranges. As shown in Fig. 4, the auxiliary state space is divided by two vertical boundary lines situated at $z_1^{1,2} = \pm\frac{\pi}{2}$ into 3 subspaces Rgn_i, $i = 1, \ldots, 3$.

Figs. 4 and 5 prove that the following chosen matrix

$$P = \begin{bmatrix} 2000 & 300 \\ 300 & 100 \end{bmatrix} \tag{47}$$

ensures that the Lyapunov function V (22) is positive in all subspaces and that the Lyapunov difference ΔV (23) is negative in each corresponding subspace. Therefore, the connection of all the auxiliary subsystems of the inverted pendulum system is stable for the obtained sliding and gain vectors.

Fig. 6 shows numerical simulation results of ODISMC using LQR approach. Figs. 6(a)-6(b) depict the state variables $x_{1,2}(k)$ and their corresponding references $x_{m1,2}(k)$. They show that the proposed controller ensures not only the stability of the closed-loop system in discrete-time sliding mode but also the follow-up of the reference model while respecting control input constraints. Fig. 6(c) illustrates the constrained control input $u(k)$. It shows that

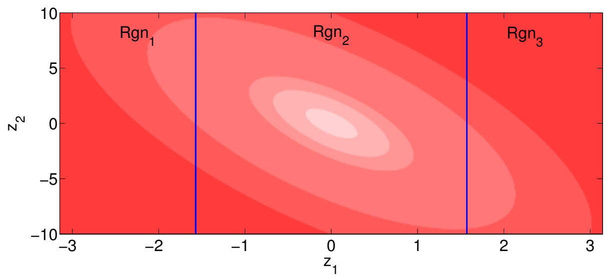

Fig. 4. The color coded values of V corresponding to each subsystem. Red color stands for positive V ; the color gradually gets lighter when V approaches zero.

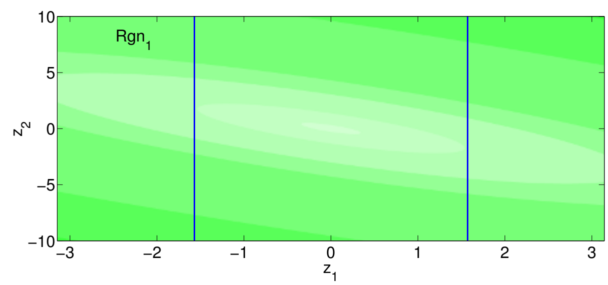

(a) Variation of ΔV in Rgn_1.

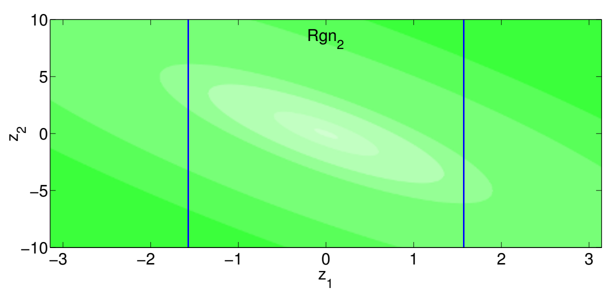

(b) Variation of ΔV in Rgn_2.

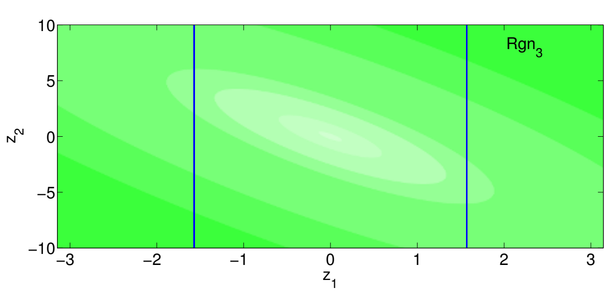

(c) Variation of ΔV in Rgn_3.

Fig. 5. The color coded values of ΔV corresponding to each subsystem. Green color stands for negative ΔV ; the color gradually gets lighter when ΔV approaches zero.

chattering phenomenon is avoided since the controller is designed on the basis of discrete-time sliding mode concept that consists in defining the equivalent control as the piecewise-constant control. Fig. 6(d) presents the sliding

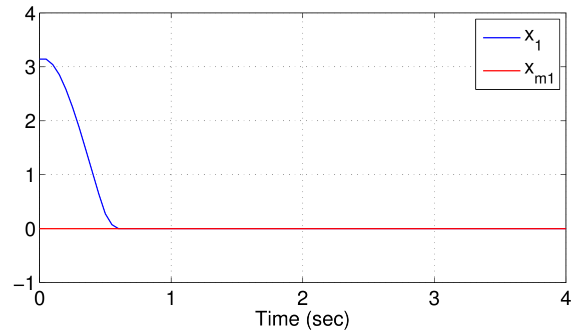

(a) State variable $x_1(k)$ and its reference $x_{m1}(k)$.

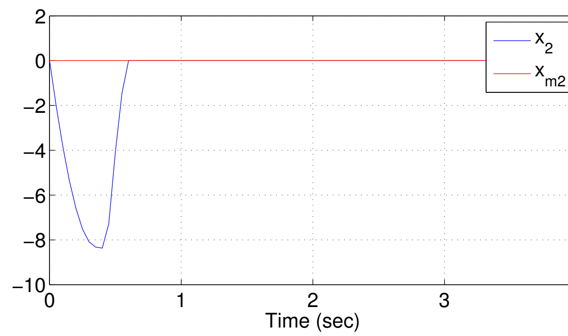

(b) State variable $x_2(k)$ and its reference $x_{m2}(k)$.

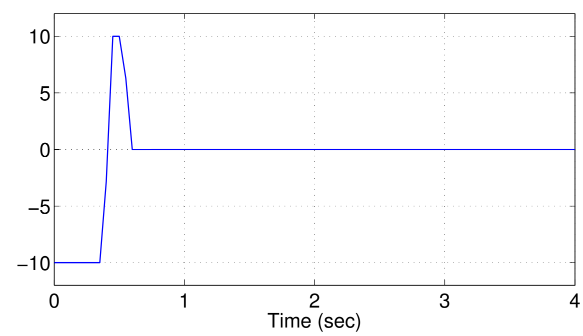

(c) Control input $u(k)$.

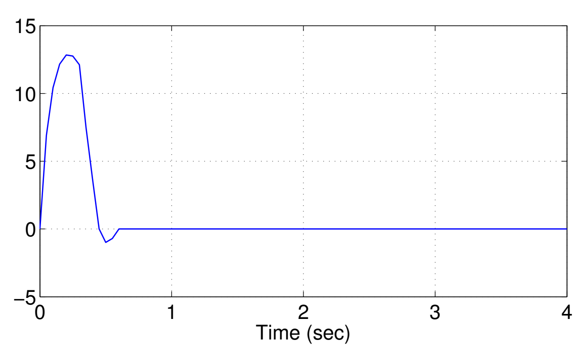

(d) Sliding function $\sigma(k)$.

Fig. 6. Simulation results of ODISMC using LQR approach.

function $\sigma(k)$. It shows that the state trajectory, which diverges at the beginning because of constraints, converges

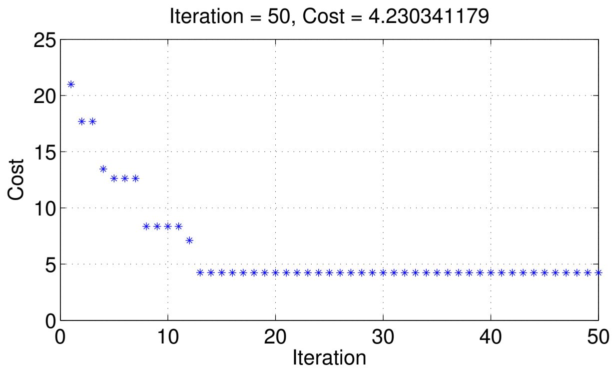

Fig. 7. Evolution of the cost function for ODISMC using LMI approach.

to the sliding surface in finite-time interval.

Using LMI approach, the auxiliary subsystem (20) is asymptotically stable in discrete-time sliding mode if there exist a positive-definite matrix $X \in \mathbb{R}^n$ and a matrix $W \in \mathbb{R}^{1\times n}$ such that the following inequality is satisfied

$$\begin{bmatrix} -X & (A_{eq}X - B_{eq}W)^T \\ A_{eq}X - B_{eq}W & -X \end{bmatrix} < 0. \tag{48}$$

The gain vector K is expressed by

$$K = WX^{-1}. \tag{49}$$

Fig. 7 illustrates the evolution of the cost function (42) for ODISMC using LMI approach. It shows that the developed DE algorithm ensures a rapid convergence to its minimum value 4.23 s. The corresponding sliding and gain vectors are respectively given by

$$\begin{cases} S_1 = \begin{bmatrix} 1.2793 & 0.5434 \end{bmatrix} & \text{if } \theta < -\frac{\pi}{2}, \\ S_2 = \begin{bmatrix} 1.7718 & 0.5 \end{bmatrix} & \text{if } |\theta| \le \frac{\pi}{2}, \\ S_3 = \begin{bmatrix} 4.8248 & 2.1035 \end{bmatrix} & \text{if } \theta > \frac{\pi}{2}, \end{cases} \tag{50}$$

and

$$\begin{cases} K_1 = \begin{bmatrix} -10.2346 & -9.5773 \end{bmatrix} & \text{if } \theta < -\frac{\pi}{2}, \\ K_2 = \begin{bmatrix} -23.7746 & -9.5773 \end{bmatrix} & \text{if } |\theta| \le \frac{\pi}{2}, \\ K_3 = \begin{bmatrix} -9.9318 & -9.5773 \end{bmatrix} & \text{if } \theta > \frac{\pi}{2}. \end{cases} \tag{51}$$

Fig. 8 illustrates a comparison of the state variable $x_1(k)$ between ODISMC using LQR and LMI approaches. It shows that the proposed controller provides better results. Thus, the optimization of the response characteristics of the closed-loop system is ensured using both DE algorithm and LQR approach.

Fig. 9 presents a comparison of the state variable $x_1(k)$ between ODISMC and DISMC. The latter uses the following sliding vectors that are chosen arbitrary

$$S_i = \begin{bmatrix} 1 & 1 \end{bmatrix}, \ i = 1, \ldots, 3. \tag{52}$$

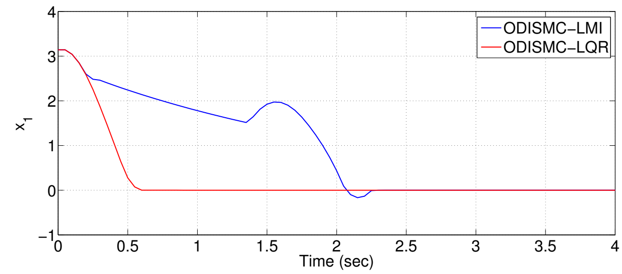

Fig. 8. Comparison between ODISMC using LQR and LMI approaches.

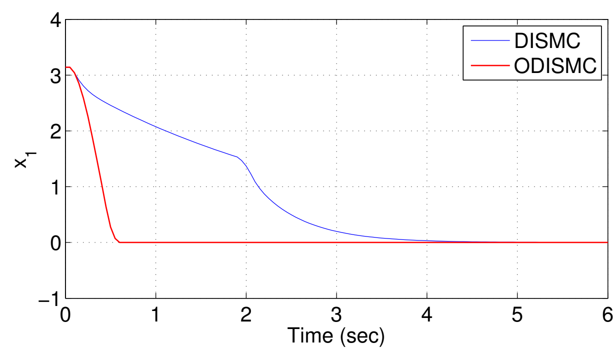

Fig. 9. Comparison between ODISMC and DISMC.

There is a notable difference between the two responses, as shown in Fig. 9. Therefore, in presence of control input constraints, the DE algorithm facilitates the determination of sliding vectors for which the response characteristics of the closed-loop system are optimum.

Fig. 10 shows a comparison between ODISMC and DISMC using LMI and LQR approaches. Referring to [32], the DISMC controller is developed without taking into account the constraints on control input. The corresponding auxiliary control law is given by

$$\begin{aligned} v(k) = & K_i z(k) - (S_iB_i)^{-1} S_i f_i + (S_iB_i)^{-1} \varepsilon(k) \\ & + (S_iB_i)^{-1} S_i \exp(-\beta(k+1))z(0) \\ & + (S_iB_i)^{-1} \varphi\sigma(k), \end{aligned} \tag{53}$$

where the design parameter $0 < \varphi < 1$ is chosen equal to 0.5 and the sliding vectors S_i are given in (52).

Fig. 10(a) presents a comparison of the state variable $x_1(k)$. It shows that the developed controller ensures the fastest response even in the presence of input constraints. Fig. 10(b) illustrates a comparison of the control input $u(k)$. It shows that the control inputs corresponding to DISMC controller using LMI and LQR methods go beyond the bounds with minimum values of -16.4 Nm and -14.2 Nm, respectively, which in practice may damage control devices.

Fig. 11 depicts a comparison of the state variable $x_1(k)$ between ODISMC and MPC. Actually, the MPC con-

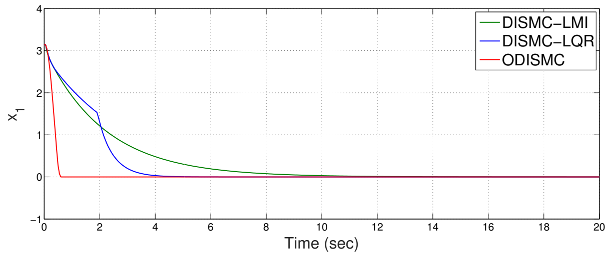

(a) Comparison of the state variable $x_1(k)$.

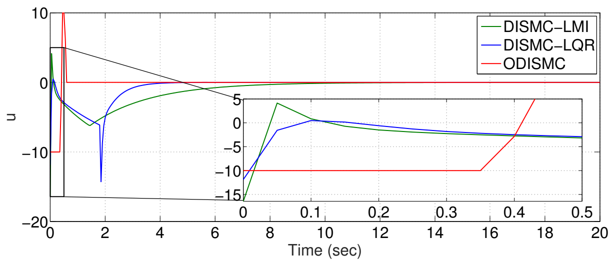

(b) Comparison of the control input $u(k)$.

Fig. 10. Comparison between ODISMC and DISMC without control input constraints.

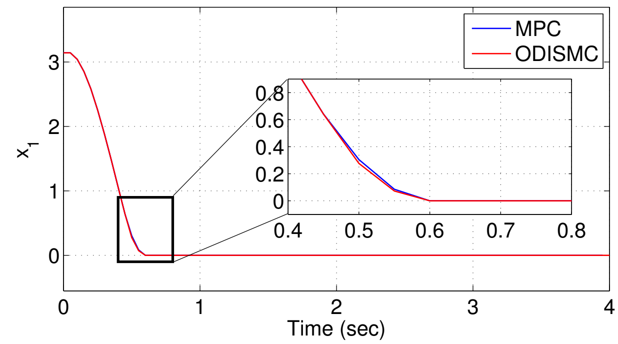

Fig. 11. Comparison between ODISMC and MPC.

troller is applied to the MLD model of the inverted pendulum system [45] and designed by minimizing the following cost function

$$\sum_{k=0}^{N_{MPC}-1} \|Q_{MPC}\left(y(k)-y_{ref}\right)\|_{\infty}+\|R_{MPC}u(k)\|_{\infty}, \quad (54)$$

where $y_{ref}=0$ is the reference signal, $N_{MPC}=5$ is the prediction horizon, and $Q_{MPC}=1$ and $R_{MPC}=0.01$ are the weighting factors. The PWA model is generated using HYSDEL (Hybrid Systems Description Language) tool [38] and then translated into MLD model. Simulation results for MPC are obtained using Hybrid Toolbox [46]. Fig. 11 shows that the two responses are very similar. Actually, the developed ODISMC, efficient to control PWA systems subject to input constraints, is a robust method that can be applied to control a class of uncertain constrained PWA systems with external bounded disturbances.

The computational costs were evaluated. Numerical simulations were performed on a standard HP Pavilion dv7 system with a 2.4 GHz Intel Core i5 CPU and a 6 GB RAM. The software platform was Matlab 2016a. The average time costs consumed by DE algorithm and the implementation of ODISMC controller are respectively about 422.094 and 4.127 seconds.

In practical applications, the developed algorithm is executed using the process model in off-line mode. Then, the sliding vectors that correspond to the minimum value of the cost function of DE algorithm will be used in the design of the controller that will be implemented in on-line mode.

5. CONCLUSION

This paper presented an optimal discrete-time integral sliding mode control for piecewise affine systems. In presence of control input constraints, the developed controller uses the differential evolution algorithm and the linear quadratic regulator approach to determine respectively the sliding and the gain vectors for which the response characteristics of the closed-loop system are optimum. Moreover, it guarantees the stability of the overall system in discrete-time sliding mode as well as the follow-up of the reference model. Based on discrete-time sliding mode concept, chattering phenomenon is eliminated and finite-time convergence to the sliding surface is ensured. Simulation results show the efficiency of the proposed scheme applied to the inverted pendulum system.

Future work will focus on extending the developed algorithm to control multi-input multi-output, disturbed [40, 47] and uncertain piecewise affine systems [41]. Future research will also focus on developing this method for Takagi-Sugeno fuzzy dynamic systems [48] and for networked systems subject to network-induced limitations such as time-delays and packet dropouts [49].

REFERENCES

[1] R. L. Grossman, A. Nerode, A. P. Ravn, and H. Rischel, *Hybrid Systems*, Springer-Verlag, Berlin Heidelberg, 1993.

[2] W. P. M. H. Heemels, J. M. Schumacher, and S. Weiland, "Linear complementarity systems," *SIAM Journal on Applied Mathematics*, vol. 60, no. 4, pp. 1234-1269, March 2000.

[3] A. J. van der Schaft and J. M. Schumacher, "Complementarity modeling of hybrid systems." *IEEE Trans. on Automatic Control*, vol. 43, no. 4, pp. 483-490, April 1998.

[4] A. Bemporad and M. Morari, "Control of systems integrating logic, dynamics, and constraints," *Automatica*, vol. 35, no. 3, pp. 407-427, March 1999.

[5] E. Sontag, "Nonlinear regulation: the piecewise linear approach," *IEEE Trans. on Automatic Control*, vol. 26, no. 2, pp. 346-358, April 1981.

[6] B. De Schutter and T. Van den Boom, "On model predictive control for max-min-plus-scaling discrete event systems," *Control Systems Engineering*, October 2000.

[7] E. D. Sontag, "Interconnected automata and linear systems: a theoretical framework in discrete-time," *Hybrid Systems III: Verification and Control*, Springer-Verlag, Berlin Heidelberg, pp. 436-448, 1996.

[8] A. Bemporad, G. Ferrari-Trecate, and M. Morari, "Observability and controllability of piecewise affine and hybrid systems," *IEEE Trans. on Automatic Control*, vol. 45, no. 10, pp. 1864-1876, October 2000.

[9] W. P. M. h. Heemels, B. De Schutter, and A. Bemporad, "Equivalence of hybrid dynamical models," *Automatica*, vol. 37, no. 7, pp. 1085-1091, July 2001.

[10] P. Biswas, P. Grieder, J. Löfberg, and M. Morari, "A survey on stability analysis of discrete-time piecewise affine systems," *IFAC Proceedings Volumes*, vol. 38, no. 1, pp. 283-294, 2005.

[11] D. Mignone, G. Ferrari-Trecate, and M. Morari, "Stability and stabilization of piecewise affine and hybrid systems: an LMI approach," *Proc. of the 39th Conf. Decision and Control*, vol. 1, pp. 504-509, 2000.

[12] G. Ferrari-Trecate, M. Muselli, D. Liberati, and M. Morari, "Identification of piecewise affine and hybrid systems," *Proc. of the 2001 American Control Conference*, Vol. 5, pp. 3521-3526, 2001.

[13] G. Ferrari-Trecate, M. Muselli, D. Liberati, and M. Morari, "A clustering technique for the identification of piecewise affine systems," *Automatica*, vol. 39, no. 2, pp. 205-217, February 2003.

[14] F. Borrelli, *Constrained Optimal Control of Linear and Hybrid Systems*, Springer, 2003.

[15] D. Q. Mayne and S. Raković, "Model predictive control of constrained piecewise affine discrete-time systems," *International Journal of Robust and Nonlinear Control*, vol. 13, no. 3-4, pp. 261-279, February 2003.

[16] C. Milosavljevic, "General conditions for the existence of a quasi-sliding mode on the switching hyperplane in discrete variable structure systems," *Automation and Remote control*, vol. 46, no. 3, pp. 307-314, March 1985.

[17] S. V. Drakunov and V. I. Utkin, "On discrete-time sliding modes," *Nonlinear Control Systems Design*, pp. 273-278, June 1989.

[18] K. Furuta, "Sliding mode control of a discrete system," *Systems & Control Letters*, vol. 14, no. 2, pp. 145-152, February 1990.

[19] W. Gao, Y. Wang, and A. Homaifa, "Discrete-time variable structure control systems," *IEEE Trans. on Industrial Electronics*, vol. 42, no. 2, pp. 117-122, April 1995.

[20] G. Golo and Č. Milosavljević, "Robust discrete-time chattering free sliding mode control," *Systems & Control Letters*, vol. 41, no. 1, pp. 19-28, September 2000.

[21] S. Z. Sarpturk, Y. Istefanopulos, and O. Kaynak, "On the stability of discrete-time sliding mode control systems," *IEEE Trans. on Automatic Control*, vol. 32, no. 10, pp. 930-932, October 1987.

[22] V. Utkin, "Variable structure systems with sliding modes," *IEEE Trans. on Automatic control*, vol. 22, no. 2, pp. 212-222, April 1977.

[23] K. D. Young, V. I. Utkin, and U. Ozguner, "A control engineer's guide to sliding mode control," *Proc. 1996 IEEE International Workshop on Variable Structure Systems (VSS'96)*, pp. 1-14, 1996.

[24] B. Bandyopadhyay, F. Deepak, and K. S. Kim, *Sliding Mode Control Using Novel Sliding Surfaces*, Springer-Verlag, Berlin Heidelberg, 2009.

[25] O. Jedda, J. Ghabi, and A. Douik, "Sliding mode control of an inverted pendulum," *Applications of Sliding Mode Control*, Springer, Singapore, pp. 105-118, 2017.

[26] G. Bartolini, A. Ferrara, and V. I. Utkin, "Adaptive sliding mode control in discrete-time systems," *Automatica*, vol. 31, no. 5, pp. 769-773, May 1995.

[27] K. Abidi, J. X. Xu, and Y. Xinghuo, "On the discrete-time integral sliding-mode control," *IEEE Trans. on Automatic Control*, vol. 52, no. 4, pp. 709-715, April 2007.

[28] V. Utkin and J. Shi, "Integral sliding mode in systems operating under uncertainty conditions," *Proc. of the 35th Conf. Decision and Control*, vol. 4, pp. 4591-4596, 1996.

[29] M. C. Pai, "Discretetime variable structure control for robust tracking and model following," *Journal of the Chinese Institute of Engineers*, vol. 31, no. 1, pp. 167-172, 2008.

[30] M. C. Pai, "Robust tracking and model following of uncertain dynamic systems via discrete-time integral sliding mode control," *International Journal of Control, Automation and Systems*, vol. 7, no. 3, pp. 381-387, May 2009.

[31] M. C. Pai, "Robust discrete-time sliding mode control for multi-input uncertain time-delay systems," *Proceedings of the Institution of Mechanical Engineers, Part I: Journal of Systems and Control Engineering*, vol. 226, no. 7, pp. 927-935, June 2012.

[32] M. C. Pai, "Discrete-time sliding mode control for robust tracking and model following of systems with state and input delays," *Nonlinear Dynamics*, vol. 76, no. 3, pp. 1769-1779, January 2014.

[33] R. Storn and K. Price, "Differential evolution a simple and efficient heuristic for global optimization over continuous spaces," *Journal of Global Optimization*, vol. 11, no. 4, pp. 341-359, December 1997.

[34] A. K. Qin, V. L. Huang, and P. N. Suganthan, "Differential evolution algorithm with strategy adaptation for global numerical optimization," *IEEE Trans. on Evolutionary Computation*, vol. 13, no. 2, pp. 398-417, April 2009.

[35] A. W. Mohamed, H. Z. Sabry, and M. Khorshid, "An alternative differential evolution algorithm for global optimization," *Journal of Advanced Research*, vol. 3, no. 2, pp. 149-165, April 2012.

[36] J. Tvrdk, "Competitive differential evolution and genetic algorithm in GA-DS toolbox," *Technical Computing Prague, Praha, Humusoft*, pp. 99-106, 2006.

[37] A. D. Lilla, M. A. Khan, and P. Barendse, "Comparison of differential evolution and genetic algorithm in the design of permanent magnet generators," *Proc. of IEEE International Conference on Industrial Technology (ICIT)*, pp. 266-271, 2013.

[38] F. D. Torrisi and A. Bemporad, "HYSDEL-a tool for generating computational hybrid models for analysis and synthesis problems," *IEEE Trans. on Control Systems Technology*, vol. 12, no. 2, pp. 235-249, March 2004.

[39] F. J. Christophersen, *Optimal Control of Constrained Piecewise Affine Systems*, Springer, 2007.

[40] E. C. Kerrigan and D. Q. Mayne, "Optimal control of constrained, piecewise affine systems with bounded disturbances," *Proc. of the 41st Conf. Decision and Control*, vol. 2, pp. 1552-1557, 2002.

[41] J. Qiu, Y. Wei, and L. Wu, "A novel approach to reliable control of piecewise affine systems with actuator faults," *IEEE Trans. on Circuits and Systems II: Express Briefs*, vol. 64, no. 8, pp. 957-961, August 2017.

[42] T. H. Hopp and W. E. Schmitendorf, "Design of a linear controller for robust tracking and model following," *Journal of Dynamic Systems, Measurement, and Control*, vol. 112, no. 5, pp. 552-558, December 1990.

[43] K. K. Shyu and Y. C. Chen, "Robust tracking and model following for uncertain time-delay systems," *International Journal of Control*, vol. 62, no. 3, pp. 589-600, 1995.

[44] S. Das, A. Abraham, and A. Konar, "Particle swarm optimization and differential evolution algorithms: technical analysis, applications and hybridization perspectives," *Advances of Computational Intelligence in Industrial Systems*, Springer-Verlag, Berlin Heidelberg, pp. 1-38, 2008.

[45] C. E. Garcia, D. M. Prett, and M. Morari, "Model predictive control: theory and practicea survey," *Automatica*, vol. 25, no. 3, pp. 335-348, May 1989.

[46] A. Bemporad, Hybrid Toolbox-User's Guide, 2003.

[47] S. V. Rakovic, P. Grieder, M. Kvasnica, D. Q. Mayne, and M. Morari, "Computation of invariant sets for piecewise affine discrete time systems subject to bounded disturbances," *In 43rd Conf. on Decision and Control (CDC)*, vol. 2, pp. 1418-1423, 2004.

[48] J. Qiu, H. Tian, Q. Lu, and H. Gao, "Nonsynchronized robust filtering design for continuous-time TS fuzzy affine dynamic systems based on piecewise Lyapunov functions," *IEEE Trans. on Cybernetics*, vol. 43, no. 6, pp. 1755-1766, December 2013.

[49] J. Qiu, H. Gao, and S. X. Ding, "Recent advances on fuzzy-model-based nonlinear networked control systems: A survey," *IEEE Trans. on Industrial Electronics*, vol. 63, no. 2, pp. 1207-1217, February 2016.

Olfa Jedda is a Ph.D. student in Electrical Engineering at National Engineering School of Monastir, Univesity of Monastir, Tunisia. She received the Engineer's degree in Electrical Engineering from National Engineering School of Monastir in 2013. Her current research interests include sliding mode control, hybrid systems and optimization techniques.

Ali Douik was born in Tunis, Tunisia. He received his B.S., M.S., and Ph.D. degrees in Electrical Engineering from the ENSET and ESSTT of Tunis, Tunisia, in 1988, 1990, and 1996, respectively and the HDR in Electrical Engineering from the University of Monastir, Monastir, Tunisia in 2010. He was in National Engineering School of Monastir from September 1991 to September 2014 and actually he is a full Professor in Computer Science department at National Engineering School of Sousse. His research interests include Automatic control, sliding mode control, Optimization, Evolutionary algorithms and Digital Image Processing.